We are IntechOpen,
the world's leading publisher of
Open Access books
Built by scientists, for scientists

6,900
Open access books available

186,000
International authors and editors

200M
Downloads

Our authors are among the

154
Countries delivered to

TOP 1%
most cited scientists

12.2%
Contributors from top 500 universities

CLARIVATE ANALYTICS
BOOK CITATION INDEX
INDEXED

WEB OF SCIENCE™

Selection of our books indexed in the Book Citation Index
in Web of Science™ Core Collection (BKCI)

Interested in publishing with us?
Contact book.department@intechopen.com

Numbers displayed above are based on latest data collected.
For more information visit www.intechopen.com

Three-Dimentional Textile Preform Using Advanced Textile Technologies for Composite Manufacturing

Peng Wang, Xavier Legrand and Damien Soulat

Additional information is available at the end of the chapter

Abstract

Textile reinforcement structure plays an important role in the reinforcement/composite performances during the composite manufacturing and in-service life of the composite material. Structures with a three-dimensional (3D) fiber topology are desired due to their superior multiaxial performance and efforts have been made to modify 2D textile technologies to produce complex 3D shapes. Most of these 3D solutions are based on the principle of adding out-of-plane reinforcements to a planar 2D fabric. Well-established 3D textile methods such as braiding and knitting have also been demonstrated to directly produce near net-shape structures. To understand these potentialities, the first section of this chapter will present the several textile technologies with strengths and weaknesses of these processes to manufacture technical reinforcements for composite applications. In the following sections, several applications with specific textile architectures will be given, in particular, the applications of the through-the-thickness reinforcement and 3D textile ply during the composite manufacturing.

Keywords: textile reinforcement, 3D fabric, tufting, 3D surface weaving, forming

1. Introduction

The definition of textile reinforcement is an essential factor during composite manufacturing and for the performance of composite material. The step of the impregnation of the reinforcement is governed by its porosity (size and distribution) [1]. Porosities can be controlled by the permeability defined as the ability of the reinforcement to transmit fluids [2]. Permeability behavior of reinforcing textiles is a strong function of the textile's complex architecture [3] and depends on the fiber volume fraction. For the specifications of composite materials, load transfer from the matrix to the reinforcement is governed by the fiber orientation, which plays a paramount role

in the composite stiffness [4]. Fiber direction and fiber volume fraction must be managed during the manufacturing process of composite materials. Resin transfer molding (RTM) [5] is one of the main manufacturing processes to produce composite parts for the transport industries [6].

A lot of experimental and numerical studies [7–11] concerning the draping stage of dry reinforcement, the first step of RTM process, were carried out to analyze the deformability of different reinforcements on specific tools. Research works have been published about the textile composite forming of hemispherical [12, 13], double-dome [14], tetrahedral shapes [15], and also with square box [16]. On these complex shapes, this preforming stage modifies the main parameters as fiber direction and fiber volume fraction and consequently has a significant influence on the resin flow impregnation and on the characteristics of the final composite part. The behavior of highly aligned reinforcements (woven, braided knitted, etc.) during the preforming step is characterized by complex coupled tensile, in-plane shear, and bending, but also by compaction deformations. Criteria to define the feasibility to realize a particular shape are based on limits of these deformations, such as the locking angle [17] for the in-plane shear behavior. All these studies have shown that the reinforcement architecture is a main parameter to predict the feasibility forming conditions and to prevent the manufacturing defects.

During the manufacturing of composite parts, defects may be introduced in their structure. Potter et al. [18] have presented a taxonomy of defect states that may have adverse impacts on the performance of composite parts. During the first step of the RTM process (preforming stage), with the use of full-field optical measurements of strains, the detection of defects is possible, as wrinkles [19], nonhomogeneity of the fiber density, and if the discontinuity of the preform due to sliding of tows takes place. The quantification of different level of strains in tension or in-plane shear can be also analyzed for the mechanical state of the preform. At mesoscopic scale, tows misalignment in the plane of the fabric or tow buckles that are defined as out-of-plane misalignment [20, 21] can be investigated. This presentation of defects could not be complete without mentioning the difficulties associated to the preforming of multilayer dry textile reinforcement, or thick as preforms as those used in high-tech industrial domains, such as automotive and aerospace industries, for instance, fan blades developed by Snecma [22]. In the literature, the preforming of multilayer dry textile reinforcements has been one of the main subjects [10, 11, 23]. In the considered forming parameters of multilayers, the number and the orientation of each ply must be taken into account. The study presented in Ref. [8] shows that preforming of multilayer is not yet controlled and demonstrate the influence of the layer orientations especially on the draw-in and finally on the final shape. The interply behavior is used, for example, with the identification of friction laws, through numerical and experimental studies [24, 25]. However, these studies estimated criteria of forming only on the top or bottom ply and did not measure the quantities in each ply of the multilayer. When these defects manifest during forming applications (and also thermostamping [23, 26]), it can be controlled by the addition of lateral restraint (e.g., matched die) or modification of forming temperature, tooling velocity, contact-to-free edge distance (e.g., blank size), and pretensioning (e.g., binder pressure) [27, 28]. Parametric studies are developed to study independently the effect of each of these parameters on final part quality; especially, experimental approaches lead to well understand the influence of the processing conditions to fabricate defect-free preform, as for example, the effect of blank-holder [29]. The development of numerical tools, by finite element simulation, can be an effective approach to take into account whole coupling parameters, to avoid experimental trial and error, and finally define optimal

configurations of these parameters. If research works were concerned the efficiency of the modification of forming process parameters to avoid/reduce these defects, the influence of specifically the nature and the architecture of dry preform during the preforming is less analyzed.

Studies concerning, separately, the preforming of carbon, glass, and also natural fiber textiles in woven fabrics [12], nonwoven fabrics [30], noncrimp fabrics [24, 31], three-dimensional (3D) interlock [12, 32], weft-knitted fabric [25], UD [33], or also braided reinforcements [34] can be found in the literature. These studies show that there is a very wide range of types of reinforcements from high performance fibers such as carbon, glass, or aramid fibers to natural or hybrid (as comingled [35]) fibers, which can be used to manufacture composite materials [36]. These reinforcements are developed from textile technologies, as weaving, knitting, breading, or nonwoven manufacturing processes, and have different mechanical properties, especially during the preforming step. The classification of these reinforcement architectures, in the textile literature, is based first on the technologies used but also on the fiber topology, e.g., the number of fiber directions [37, 38], but conventional laminated composite has fibers oriented only in the plane of the laminate and is therefore vulnerable to delamination. Due to the inclusion of the through-thickness yarns, three-dimensional (3D) fiber reinforced composites have several advantages over traditional two-dimensional (2D) composites such as elevated fracture toughness, better interlaminar fracture toughness, higher damage tolerance, impact resistance, and tensile strain-to-failure [39]. Due to the complexity and diversity [40] of these 3D composite architectures [41], the performance and efficacy of these 3D composite in service are predicted early from numerical computational work. In order to validate the computational results and gauge the influence of the through-thickness fibers on the in-plane and out-plane mechanical properties, numerous authors have worked on the identification of the mechanical properties of 3D reinforced composites [42]. Transverse cracking and propagation of delamination have been studied earlier with the help of digital image correlation (DIC), which maps the surface strain distribution [43]. Moreover, to describe the complex 3D preform architecture, X-ray microcomputed tomography has also been used [44]. Consequently, efforts have been made to modify 2D textile technologies to manufacture complex 3D preform [37, 38]. Most of these 3D solutions are based on the principle of adding out-of-plane reinforcements to a planar 2D fabrics, examples include z-pinning [45], interlock-weaving [46], stitching [47], or tufting [48].Well-established 3D textile methods such as braiding [49], weaving [40, 46], and knitting [50] have also been demonstrated to directly produce near net-shape structures. The control of these textile technologies that are able to manufacture 3D preform is absolutely necessary to avoid damage occurring by the insertion of the through-the-thickness reinforcement and consequently decreasing mechanical properties of 3D composites.

To describe potentialities of 3D preform reinforcement especially during manufacturing steps of composite materials, this chapter focused on applications. In the second section, the several textile technologies will be presented in fact to understand architecture of reinforcements and its influences on their properties. Strengths and weaknesses of these processes will be given. In the third section of this chapter, an example of through-the-thickness reinforcement by tufting will be described specifically for the preforming step of the RTM process. Experimental comparisons between untufted and tufted samples subjected to hemispherical preforming will be compared to minimize defects as interlayer sliding or excessive draw-in. In the latest section, concerning the manufacturing of a square box part, two methods are compared: the classical preforming realized experimentally by a specific preforming device and the surface 3D weaving able to

deposit the warp and weft yarns perfectly perpendicular on all of the surfaces of the final 3D ply. Fiber orientations as well as wrinkles and in-plane shear angles are analyzed and compared for each preform obtained. Conclusions and prospects finish this chapter.

2. Classification of preform architecture

Several points need to be remembered to introduce textile reinforcement classifications. (1) In a composite material, the fiber contributes mainly to the mechanical performances of the final parts. The positions and orientations of the fibers are critical to the mechanics of final parts. (2) The textile structure and the composite part should be distinguished. The textile structure is so-called dry: it is a semiproduct. The composite part is composed of the impregnated textile structure of polymerized matrix or reconsolidated matrix. (3) Textile structures are fundamentally multiscale materials in which the macroscopic mechanical behavior of the structure is directly inherited behavior at lower scales. Three scales of observation of the reinforcement are generally recognized (**Figure 1**): microscopic scale (scale of fiber), mesoscopic scale (scale of the tow and the structure pattern), and macroscopic scale (scale of the whole part).

The textile structures are very diverse although traditionally classified into the four main technologies: weaving, knitting, braiding, and nonwoven. There are many ways of classifying textile structures:

- by construction technology: weaving, knitting, braiding, and nonwovens according to their dimensionality: 1D, 2D, 3D,… [51]

- by number of orientations: monoaxial, biaxial,…

Different classifications have been suggested for the fiber reinforcement architecture in order to help the designer to select the architecture that respond to the cost and performance requirements. These classifications are based on the structural integrity and fiber linearity and continuity, fiber orientation, or the textile manufacturing technology. The conventional textile technologies have significantly evolved over the last century, especially by using technical fibers as glass or carbon fibers. However, some limitations are associated with the employment of conventional textile processes in technical fiber manufacturing reinforcement preforms, as the high degradation of technical fiber/yarn on the conventional textile machineries are occurring, or either, the fact that conventional machineries allow only the production of planar (2D)
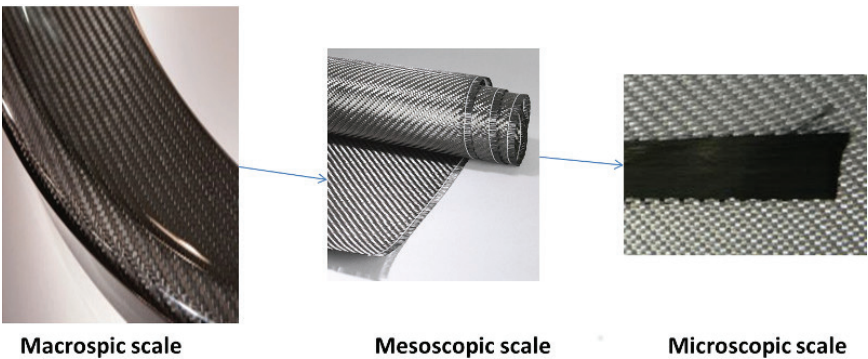

Macrospic scale   Mesoscopic scale   Microscopic scale

Figure 1. The three levels of study woven fibrous reinforcements.

or thin cylindrical preforms. It is possible to sort out the textile structures according to their size, i.e., size determined by fiber orientations.

The component of the textile structure is the fiber. It can be presented in the form of tape, roving, or yarn. The textile structure is a tangle of fibers. Let us agree that the twisted yarn or multifilament twisted or not is considered one-dimensional (1D), as in this longitudinal direction, the stiffness is predominant. Therefore, size of textile structure is drawn by mechanical stiffness orientations, i.e., along fibers. Similarly, the fabric that is obtained by nonwoven technology, by weaving, knitting, or by flat braiding is considered in 2D as the fibers are almost oriented into one plane, associated rigidities membrane. A so-called conventional 2D preform comprises fibers oriented in the main plane of the structure. For example, a conventional woven fabric, in the plane (X, Y), has fibers oriented along the X axe (said at $0°$ angle) and transverse fibers, along the Y axe (said at $90°$ angle). Therefore, none are along the Z-axis, i.e., out of the plane (X, Y). The major advantage of a so-called 3D preform is that, having fibers in the "third direction," the structure is generally more efficient because more mechanically efficient mechanically in this "third direction," as explained by Mouritz et al. [37, 47, 52–54].

Recall that the reinforcement into a composite material serves to strengthen, i.e., to provide the mechanical properties of the composite part. Moreover, one possible definition of the "size" of a textile structure is given by the orientation of the fiber bundles that constitute it. In fact, the comparison and classification of textile preforms is a difficult task because of the diversity of 3D structures as shown in **Figure 2**. Fukuta and Aoki have classified textile preforms according to different criteria such as the fiber orientation, the method of manufacture, or the geometry of the final preform (see **Figure 3**). Besides, a growing number of Z-reinforcement methods are available. Integral techniques (3D knitting, 3D weaving, or braiding) must be distinguished from insertion of the Z-reinforcement. For Z-reinforcement techniques, the insertion in Z-direction is separate manufacturing steps after the initial preform lay-up. It is the case for the structural stitching, the tufting, the Z-pinning or either the Z-anchoring. Besides, integral techniques are developed for the manufacture of large-scale 3D reinforced laminates, and Z-reinforcement techniques are ideally suited for the localized Z-reinforcement of sections in the composite with high out-of-plane stress state. A new class of reinforcements has to be introduced. Let us call it 2D+. A 2D+ structure is a structure where the thickness is greater than that of the 2D structures, but not as much as other dimensions. The 2D+ structures can be defined as structures where the thickness is greater than that of the 2D structures. For example, the woven structure called "interlock Aerotiss 2.5D" [55] is a bonding layer to chain interlock fabric layer having multiple layers in the thickness. A weave derived from the three-layer structure is carbon reinforcement, G1151, from Hexcel. Note that this structure is thicker than a simple fabric that tows bind the layers together. For interlock structures, the thickness is less negligible compared to the other dimensions and some are no longer just in the main plane (X, Y) of the structure.

In order to solve the problems associated with traditional laminated structures and especially their low interlaminar properties, much energy has been deployed in the past 50 years to develop composite structures with 3D reinforcements [37]. Many techniques can lead to the production of 3D textile architecture as 3D weaving, 3D braiding, and stitching. All these techniques are designed to obtain complex 3D shapes while providing improved mechanical performance. From all the classifications listed previously, a study of the typology of textile reinforcements is
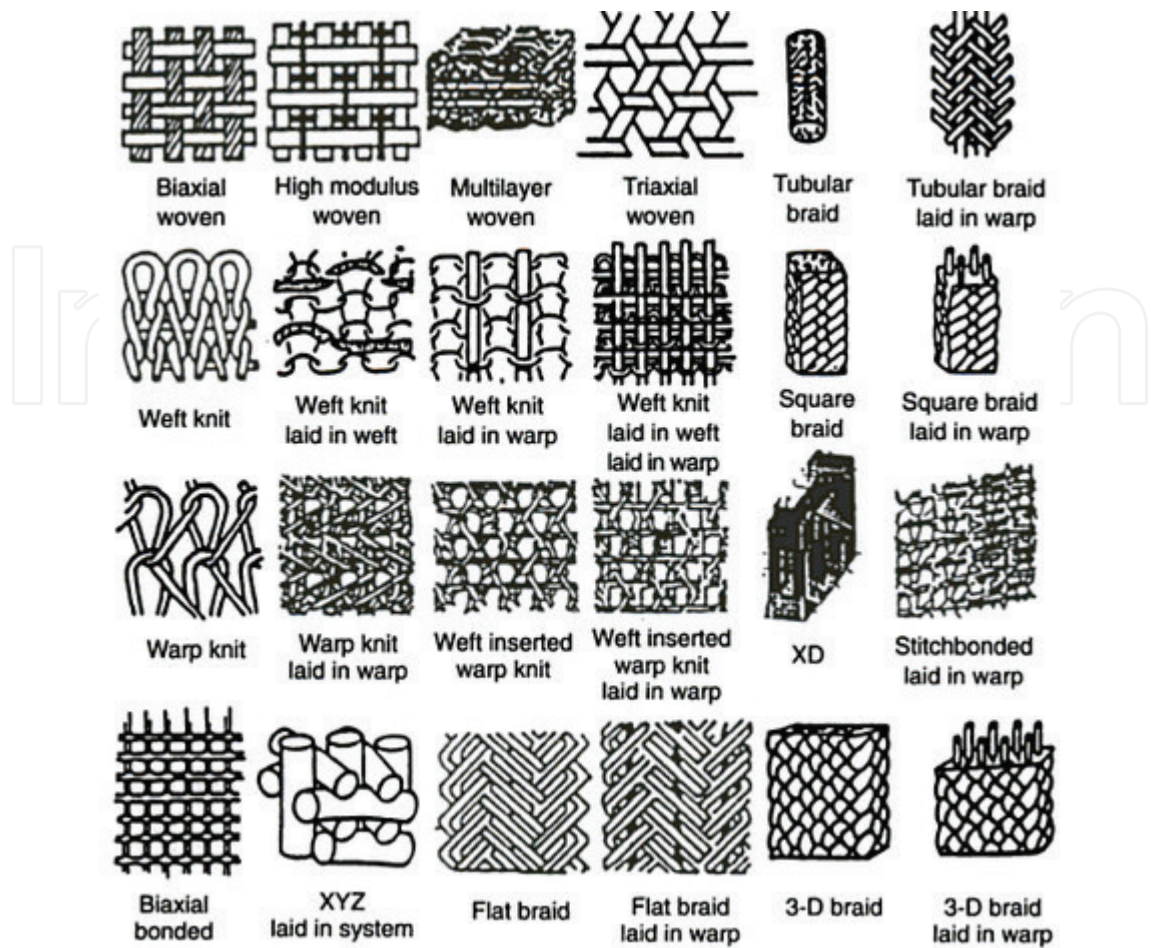
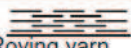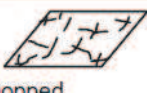**Figure 2.** List of textile structures by Ko and Du [56].
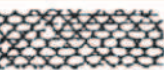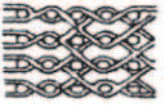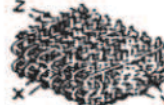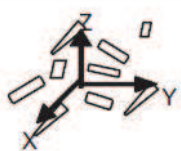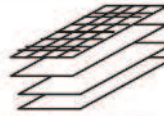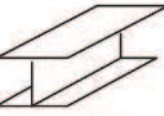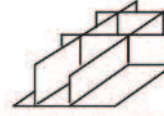
AXIS / Dimension	Non-axial	Mono-axial	Biaxial	Triaxial	Multi-axial
1D		Roving yarn			
2D	Chopped	Pre-impregnation sheet	Plane weave	Triaxial weave	Multi-axial
3D — Linear element	Strandmat	3D braid	Multi-ply WEAVE	Triaxial 3D weave	Multi-axial 3D weave
3D — Plane element		Laminate type	H or I beam	Honeycomb type	

Figure 3. Classification by Fukuta and Aoki [57].

proposed in **Figure 5** to classify preforms during the various developments. The purpose of this classification with respect to all those present in the literature is to situate new textile reinforcement structures for composites. Moreover, the classification in **Figure 5** also proposes a class for flat thick preforms as woven interlock: the 2D+ class. It makes a case for assembly preforms. These structures are 3D structured using even strengthened by assembly, whether by stitching, but also by tufting or nailing. The classification in **Figure 4** explores unnamed geometric preforms. The main aim of the proposition presented in **Figure 5** is to clarify what is called 3D. It should also help researchers to define where are set their objects.

Orientation / Dimensions	randomly	mono axial	bi axial	tri axial	multi axial
1D	fibre	tow, yarn			
2D	non woven	uni directional	Fabric: Woven, knitting, bi axial braiding	tri axial braiding: flat, over braid	NCF stitch bonded, NCF woven
2D+	thick non woven		woven interlock	multi axial multi-layer interlock	
3D — surface	shaped non woven		tetrahedron ply stamping	over-braiding, preforming, stamping of braid or/and multi axial	
3D — volume			assemblies by tufting, stitching, nailing/pinning	cross of shaped	BWS, cross of stiffeners (integral 3D)

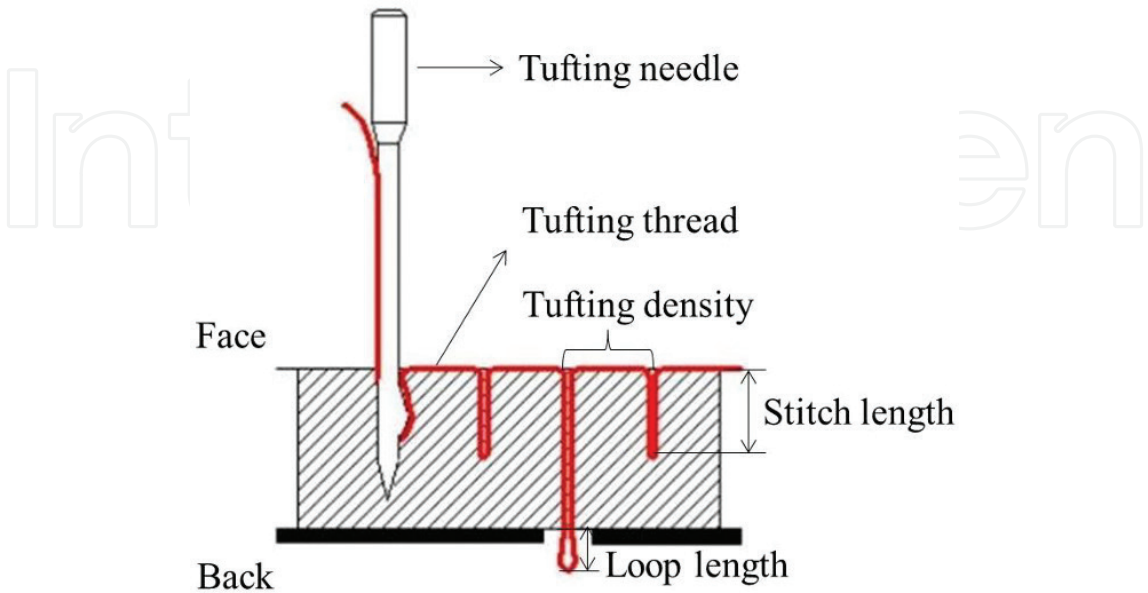Figure 4. Classification of textile preforms.

Figure 5. Tufting process.

3. Reinforcement by tufting technology

In this subdivision, an example of through-the-thickness reinforcement technology is applied and examined for its influences during the preforming stage of the RTM process. For thick composite parts, multilayer dry textile reinforcements are deformed on tools associated with the geometry of the composite part to fabricate. The interply sliding is identified as a major forming defect during this phase of the procedure. Moreover, the manufacturing defects will be presented and especially on the influence of the layer orientations on the sliding and wrinkles, which are not acceptable for the final part.

3.1. Tufting process and tufted 3D reinforcements

Tufting technology has been developed based on the stitching technique (see **Figure 5**). The dry reinforcements are tufted together by yarn loops. **Figure 5** shows a hollow needle passes through one side of dry preform without tension. When the hollow needle retracts, the tuft yarn is kept within the dry preform by friction and forms a loop. Tufting technology applies a formation of loops with a loose and almost stress-free presentation of the threading system that can bring down the stitching effect on the in-plane properties [55, 58]. Compared to the conventional stitching, tufting is much simpler as it does not require a second thread and lock the threads [58].

A specific tufting device developed in GEMTEX Laboratory is shown in **Figure 6**. **Figure 6a** shows the tufting equipment. Four principal parts of this equipment: tufting device,
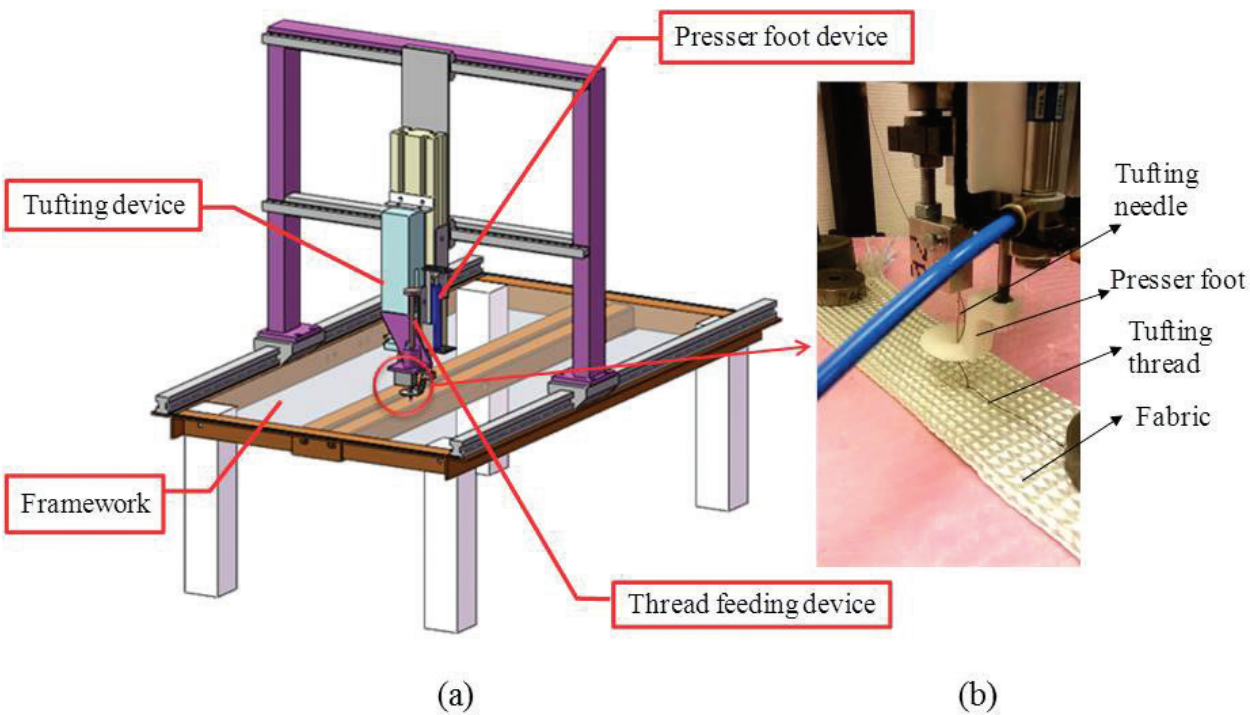

Figure 6. The tufting equipment (a) and zoom of the tufting head (b).

presser foot device, thread feeding device, and framework are illustrated. The tufting needle linked to a pneumatic jack in order to well-control the tuft length. A presser foot situated next to the needle is carried by another pneumatic jack to apply a force per unit area on the preform in tufting process. The thread feeding device provides tufting yarn with a certain length and tautness. These devices are installed along a mobile framework to form the tufting head (see **Figure 6b**). During the tufting, stitch length, tufting density, tufting direction, and pressing of the presser foot can be well-controlled. The maximum tuft length 50 mm is used in the present study, which is decided by the range of the pneumatic jack. A change of needles can be selected according to the yarn performance and the cloth of the preform.

For the presented case, the reinforcement fabric is E-glass plain weave with an area density of 157 ± 5 g/m^2. The tested preforms were first laminated with four plies $[\pm 45°, 0°/90°]^2$. **Table 1** shows the preforms were tufted by TENAX® carbon yarn with different tufting densities corresponding to a tufting spacing. The tufting spacing is defined by the vertical distance of two neighbor tuft lines. One of the preforms after tufting is shown in **Figure 7**. The dimensions of the tested preforms are $280 \times 280 \times 1.0$ mm^3. As presented in **Figure 7**, the preform is tufted in square spiral pattern to assure that the tufting thread is continuous and uninterrupted and inserted in two directions (warp and weft directions).

Ref. of samples	Area density (g/m²)	Tufting spacing (mm)
Non-tufted	626.3	-
Tufted 2.0	639.0	20
Tufted 1.0	665.8	10
Tufted 0.5	707.9	5

Table 1. Main properties of the tufted 3D fabric specimens.
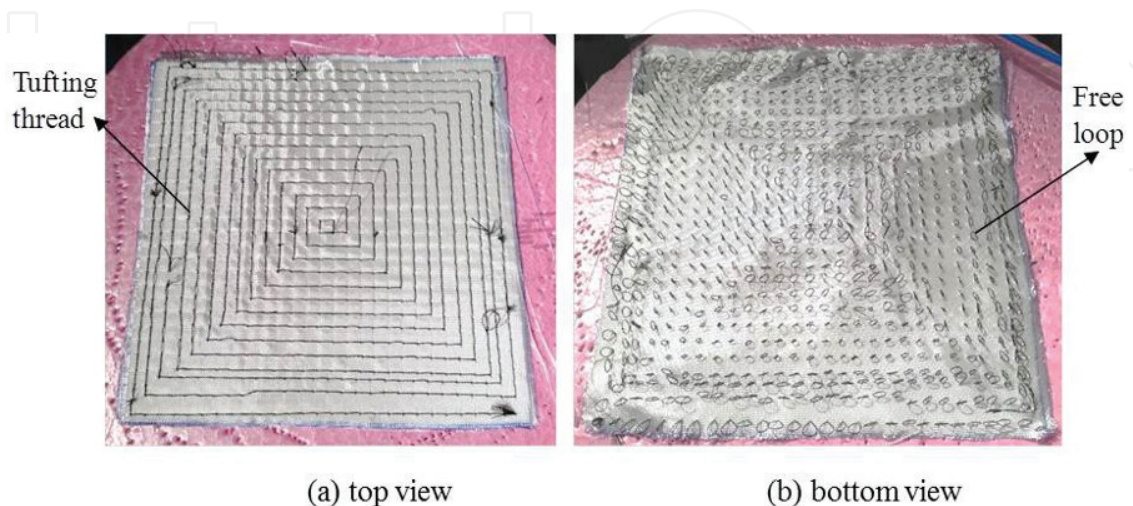

(a) top view   (b) bottom view

Figure 7. Tufted sample with a tufting spacing of 10 mm. (a) Top view; (b) bottom view.

3.2. Hemispherical forming

The hemispherical forming is performed on a specific preforming device shown in **Figure 8** [12]. The diameter of the hemispherical punch is 150 mm. The hemispherical preforming device was used to analyze the double-curved shape forming with a given textile reinforcement under different conditions (shape of punch, position, and pressure of blank-holder). The tufted 3D fabric is placed between the blank-holder and die. Four pneumatic jacks, connecting to the blank-holder, are used to set an adjustable pressure on the cloth. In order to measure the important forming parameters by optical measurement, such as the material draw-in and interlayer sliding, the open-die forming is used.

3.2.1. The multilayered reinforcement forming

In order to manufacture the thick composite parts, it is frequently used in multilayered forming [23, 59, 60]. **Figure 9** shows the shape of the E-glass plain weave preforms after the hemispherical preforming. The deformed preforms are symmetric, and there are no wrinkles that can be observed in the usefulness zone (the flat zone). The sliding is noted on the interface of plies as the plies are simply superimposed. The maximum intersliding can be measured by the difference of material draw-in between the top and the bottom plies.

3.2.2. The tufted 3D reinforcement forming

The preforming of four different tufted 3D fabrics is figured out. The forming conditions are identical to the multilayered forming presented previously (punch displacement 65 mm and blank-holder pressure 0.05 MPa). The deformed preforms are shown in **Figure 10**. The influence of tufting spacing can be followed on the different results. The tufting yarn reinforces
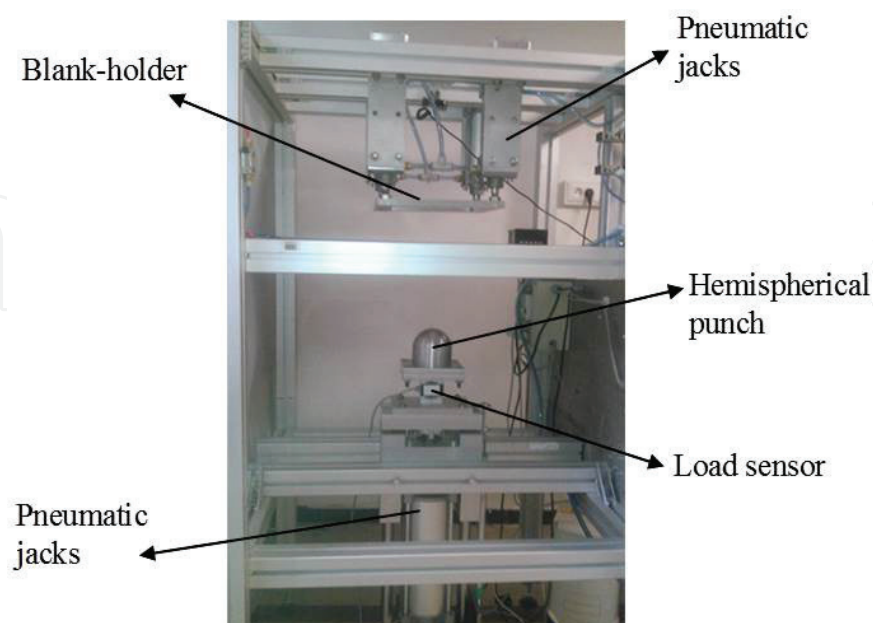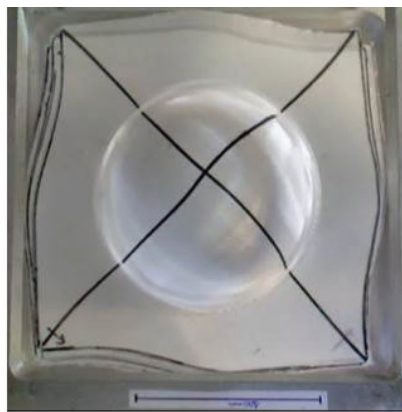

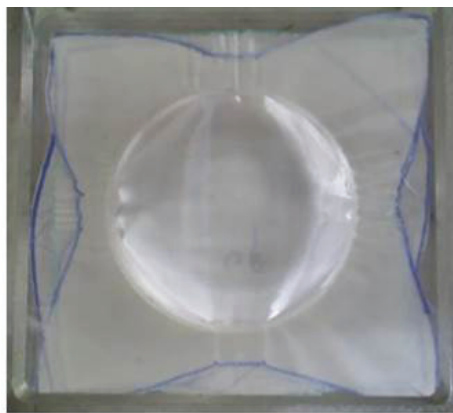**Figure 8.** The hemispherical preforming device.

(a) The preform : [0° /90°]₄   (b) The preform: [-45° /+45°]₄

Figure 9. The multilayered forming. (a) The preform [0°/90°]⁴; (b) the preform [−45°/+45°]⁴.

(a) Non-tufted   (b) Tufted 2.0

(c) Tufted 1.0   (d) Tufted 0.5

Figure 10. The different tufted 3D preforms after performing. (a) Nontuftled; (b) tufted 2.0; (c) tufted 1.0; (d) tufted 0.5.

through the thickness of the preform and then the interply sliding can be minimized. It can be observed that the tuft yarns can be broken by the interply sliding in the weak tufting density cases (for example, tufting spacing of 10 and 20 mm). Consequently, it has better to choose a rather high tufting density to reinforce the "Z" direction (for example, tufting spacing of 5 mm), but a higher tufting density leads to a heavier and more rigid preform, and as a result the forming process will be difficult to achieve.

As one of the most common defects, wrinkling can be experienced frequently in textile reinforcement forming [23, 26, 29, 61]. The possible relative motion of fibers due to the internal composition of textile reinforcement leads to a weak bending stiffness [18, 62]. Wrinkling is a global phenomenon, which depends on the strain, force components, and boundary conditions of forming process [61]. However, the wrinkling phenomenon can be modified by the use of tufting technology. Wrinkling phenomena are shown in **Figure 11** for the forming with different preform. Big wrinkles with a nonregular shape can be noted in the forming of nontufted preform (**Figure 11a**). Compared to the deformed nontufted preform, in the forming of tufted 1.0 and tufted 0.5 preforms the wrinkles are regularly distributed and the size of wrinkle is much reduced.

The influence of tufting yarn orientations is analyzed. Two plies E-glass plain weave are superposed and tufted trough-the-thickness with the different orientation of the tufting yarn (see **Figure 12**). Mass of preform is not changed as the dimensions of ply and the tufting spacing are not changed. Comparing the $[0°/90°]^2$ preforms tufted in 0°/90° and in ±45° directions, the change of tufting yarn orientations does not alter the global deformation of preform (**Figure 12**).
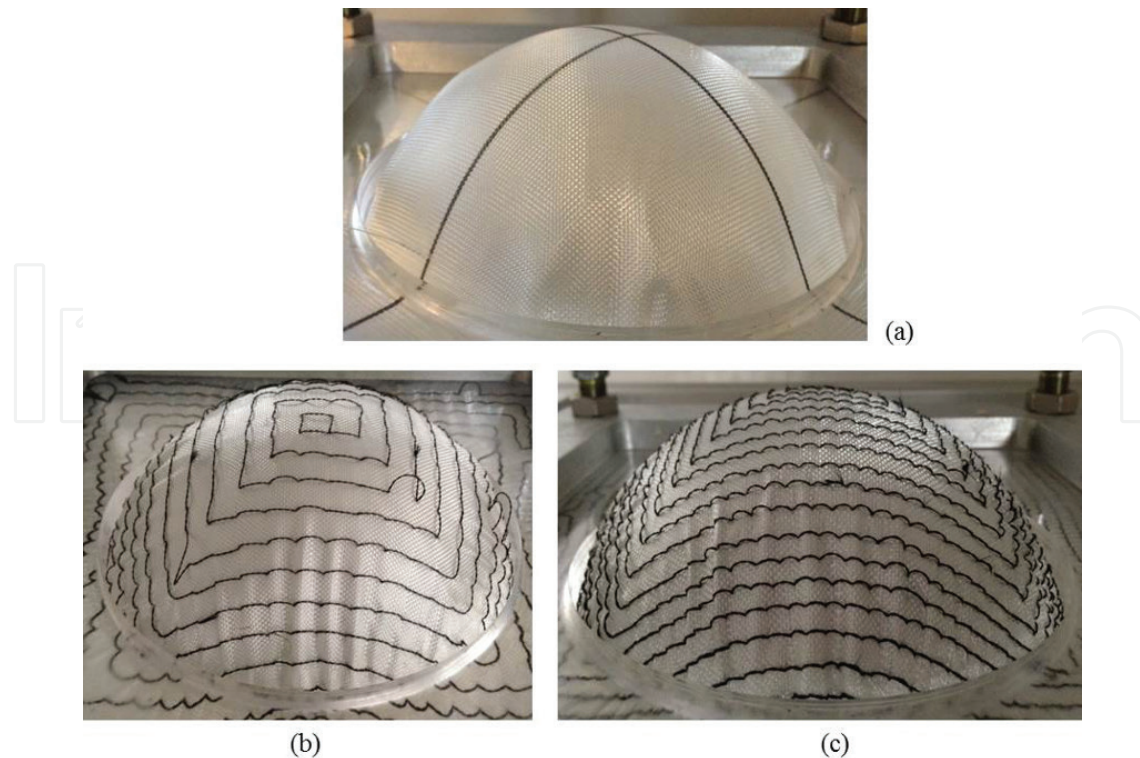

(a)

(b)   (c)

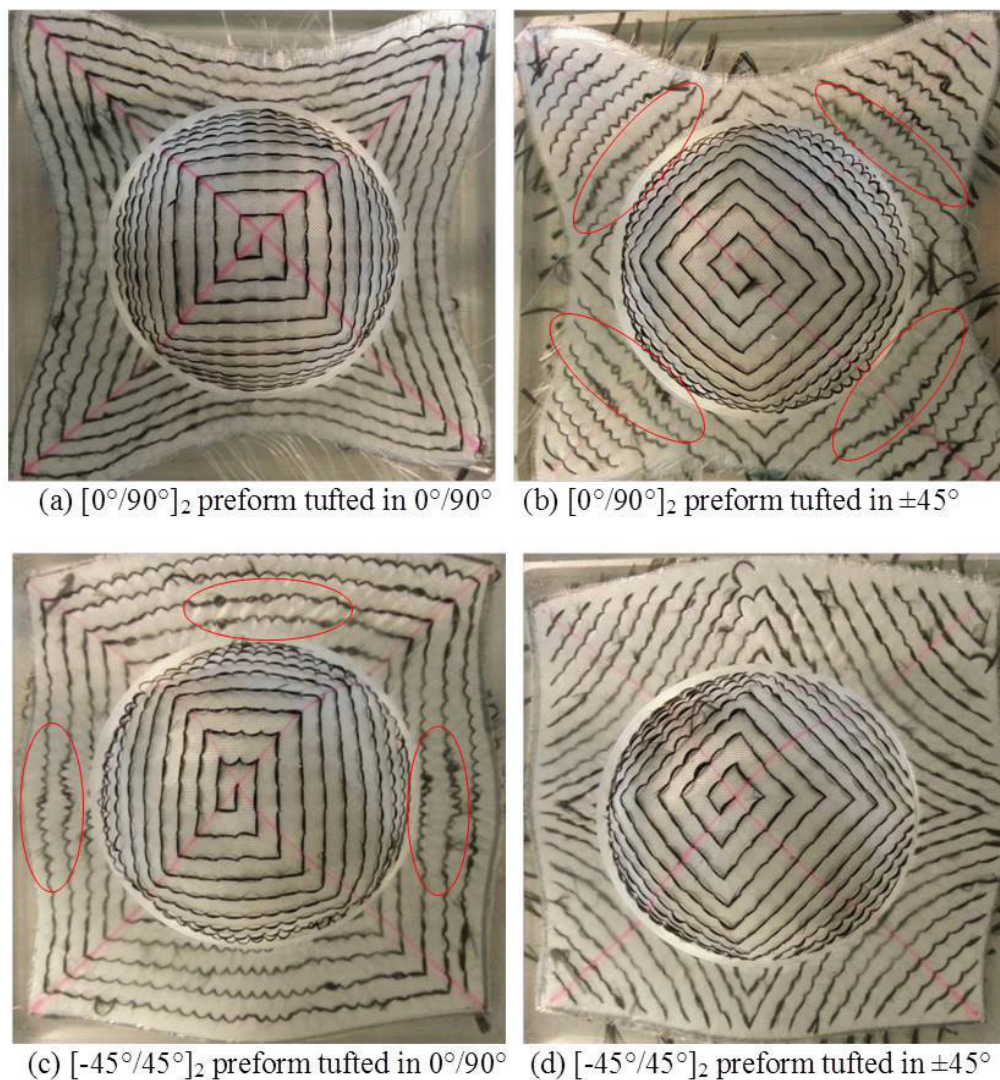**Figure 11.** Wrinkling phenomena in the forming of (a) nontufted, (b) tufted 1.0, and (c) tufted 0.5 preforms.

(a) [0°/90°]₂ preform tufted in 0°/90°   (b) [0°/90°]₂ preform tufted in ±45°

(c) [−45°/45°]₂ preform tufted in 0°/90°   (d) [−45°/45°]₂ preform tufted in ±45°

Figure 12. Hemispherical forming of different tufted 3D preforms. (a) [0°/90°]² preform tufted in 0°/90°; (b) [0°/90°]² preform tufted in ±45°; (c) [−45°/+45°]² preform tufted in 0°/90°; (d) [−45°/+45°]² preform tufted in ±45°.

As there is a strong in-plane shear effect in diagonal direction for 0°/90° ply (zones indicated on the figure), each segment of tufting thread between two tufting points is compressed and then the tufting yams in these strong shear zones are misaligned. The same phenomenon is observed in the forming of [−45°/45°]² preform tufted in 0°/90° and in ±45°. As the strong shear zones are presented in longitudinal and transversal directions in [−45°/45°] ply forming, the misalignment is noted in the deformed [−45°/45°]² preform tufted in 0°/90°(**Figure 12c**).

The influence of tufting yarns during the tufted 3D textile reinforcements forming has been investigated. The tufted preform is more rigid than the multilayered preform due to the presence of tufting yarns through-the-thickness. Hence, it requires a bigger punch force in the tufted 3D reinforcement forming. When a quasiisotropic structure [±45°, 0°/90°]² is used in the multilayered forming, a significant intersliding can be observed. In tufting process, the slippage between the plies is reduced following the increasing of tufting density. Finally, the preform can be deformed as a single 3D ply when the tufting spacing 0.5 mm is used.

4. The manufacturing process of the composite corner fitting and square box parts

As the specific parts in aeronautical and automobile applications, it is very interesting to product the composite corner fitting and square box to replace the aluminum parts. As the classical manufacturing process, the composite forming is fast and more efficient, in particular to the manufacturing of multilayer laminates and interlock fabric-reinforced composites. Forming has been developed widely for dry textile reinforcements and prepregs. As presented previously, the double-curved shape forming can possibly lead to defects; it depends strongly on the forming parameters (tool loads, blank-holder forces, temperature). A novel manufacturing technology of composite materials called the surface 3D weaving seems very promising. It demonstrates directly the geometry of final composite part without the step of 2D product. The weaving in three directions is completely designed and the warp and weft yarns stay perfectly perpendicular on all of the surfaces of the final 3D ply. It is possible by using this technique to produce the 3D composite fabrics with geometry quite complex. Compared to the traditional forming process, the surface 3D weaving is a direct route to avoid certain manufacturing defects, such as wrinkling, porosities, slippage of the network, etc. On the contrary, the 3D weaving process is long and difficult to implement.

4.1. Textile reinforcements forming

4.1.1. Corner fitting

The experimental forming with the corner fitting punch is performed on a specific preforming device presented in Section 3. The punch dimensions are shown in **Figure 13**. A woven fabric with surface dimensions of 300 × 300 mm^2 was prepared for the forming tests. The corners fitting preforming results corresponding to a 65 mm displacement of punch are shown in **Figure 14**. The warp and weft directions on the deformed plies are figured out. The preforms
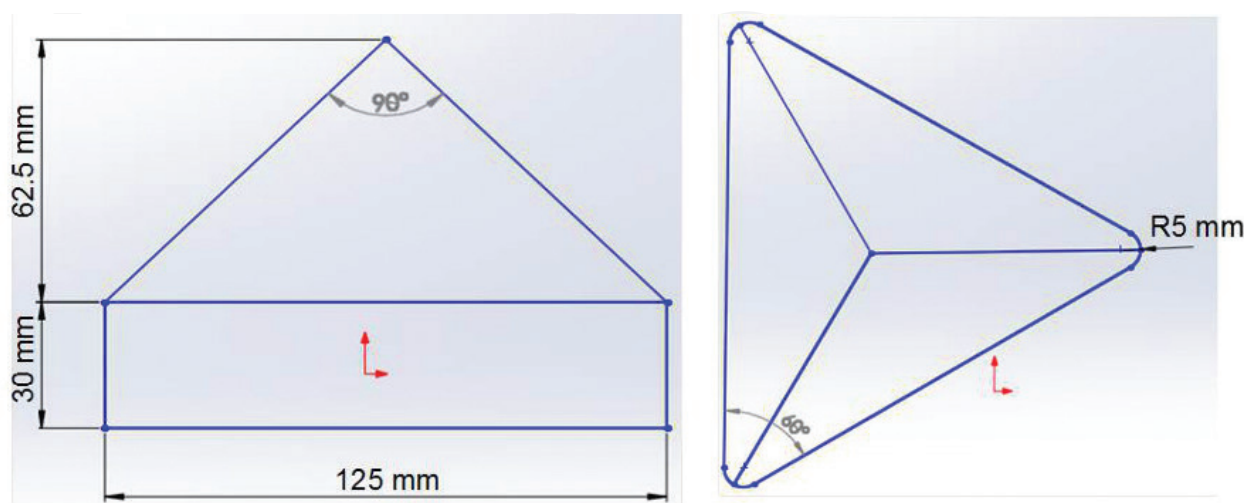

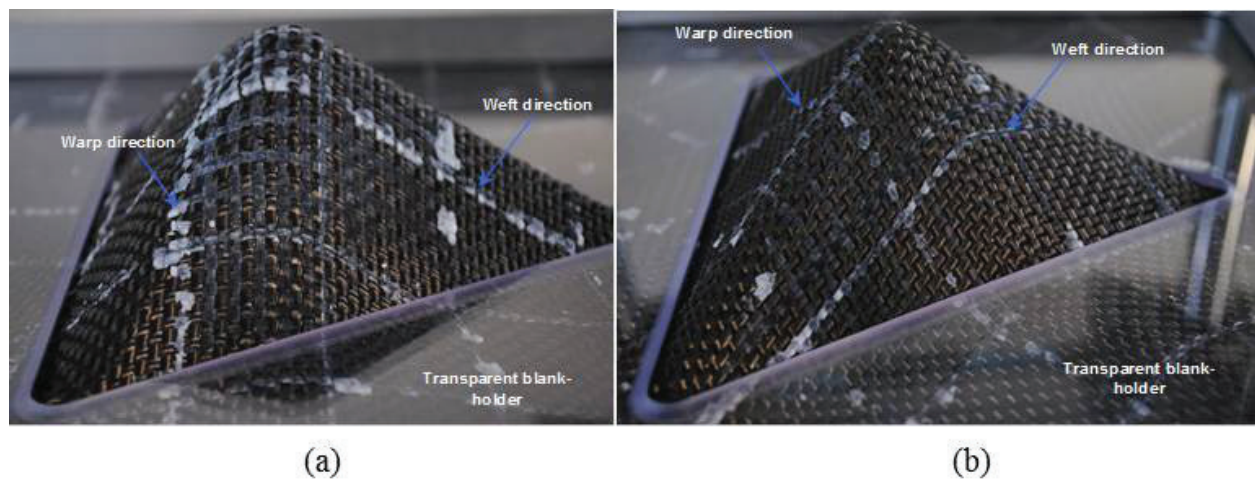
Figure 13. The punch dimensions.

Figure 14. The experimental forming with 0°/90° (a) and −45°/45° and (b) plain weave fabrics.

are obtained without defects as the rupture or the buckle of the yarns. Moreover, no wrinkling is observed in these preforming tests.

Figure 15 shows the warp and weft directions of the deformed 0°/90° and −45°/45° plies. The angle between warp and weft yarns is not constant due to different local in-plane shearing effects. There is only a small zone where warp and weft yarns are (or quasi) perpendicular on each face of deformed ply (a small zone with zero in-plane shear angle around the middle line). Furthermore, it can be observed a positive in-plane shear angle (the angle between warp and weft yarns <90°) in the left zone and a negative in-plane shear angle (the angle between warp and weft yarns >90°) in the right zone on both 0°/90° and −45°/45° deformed plies. The in-plane shear angle can reach maximum 25° after forming in both left and right zones on the deformed −45°/45° ply. On the deformed 0°/90° ply, the maximum in-plane shear angle of 25° and 20° can be observed in the left and right zones, respectively. These changes in the angle between warp and weft yarns lead to a variation of fiber volume fraction and local permeability of the textile fabric. Subsequently,
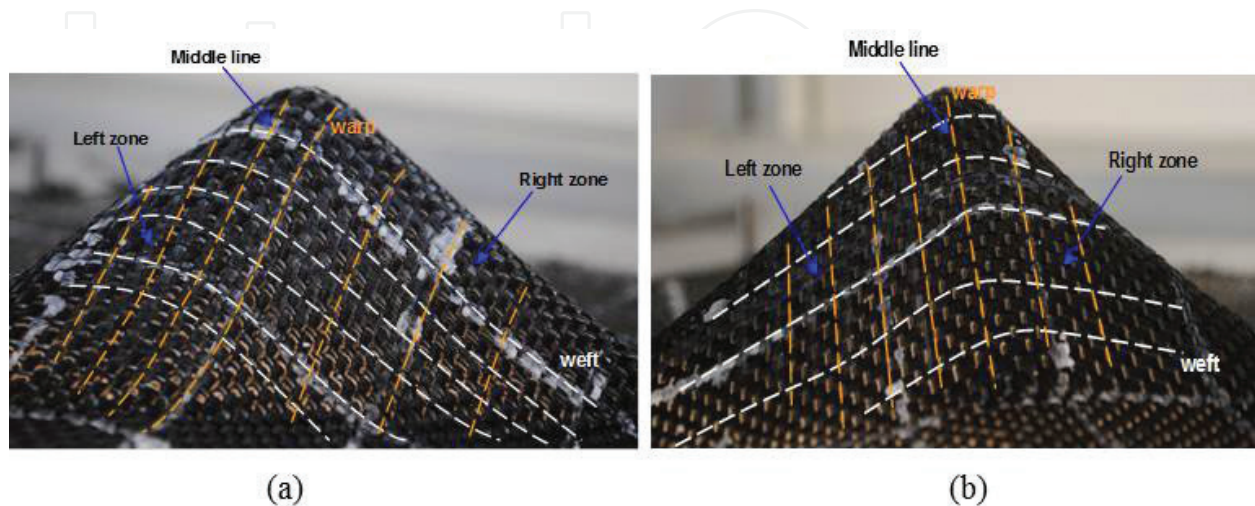

Figure 15. The yarns' directions of the deformed 0/90° ply (a) and ±45° ply (b).

it could result in a nonhomogenous flow during the resin infusion or injection stage. In this case, it will have a negative influence on mechanical performance of the final composite part. As an essential manufacturing parameter in liquid composite molding (LCM) processes, the permeability of the preform should be well controlled.

Another forming example with a tetrahedral punch performed through the numerical simulation analysis is presented in **Figure 16**. This forming simulation with a punch, as same geometry as the corner fitting part, is performed by using the approach semidiscrete [11, 23, 61]. **Figure 16a** shows the geometry of the tools (punch, die, and blank holders). The dimensions of a single ply are 425 × 425 × 0.3 mm³. Six independent blank holders are used and apply a 0.01 MPa pressure during the forming stage. **Figures 16b** and **c** present the deformed blanks and the field of in-plane shear angle obtained by the forming simulation corresponding to a 95 mm displacement of the punch. The mechanical properties of the textile fabric used in forming simulation are given in **Table 2**. The friction coefficient on the interfaces of tool/ply and ply/ply is assumed to be equal to 0.2. In the major zone of the three surfaces of corner fitting part, the in-plane shear angle is between 15° and 25°. In addition, wrinkles can be observed in the useful zone in **Figure 16b** and **c**. Wrinkling is one of the most common flaws that experiences in both dry textile fabric [61] and prepreg composites forming [23] due to the possible relative motion of fibers, internal composition of textile reinforcement, causing a very weak bending stiffness [18, 61, 63]. Wrinkling depends strongly on the geometry of the final composite parts, on the fabric characteristics and on manufacturing parameters [23, 61].
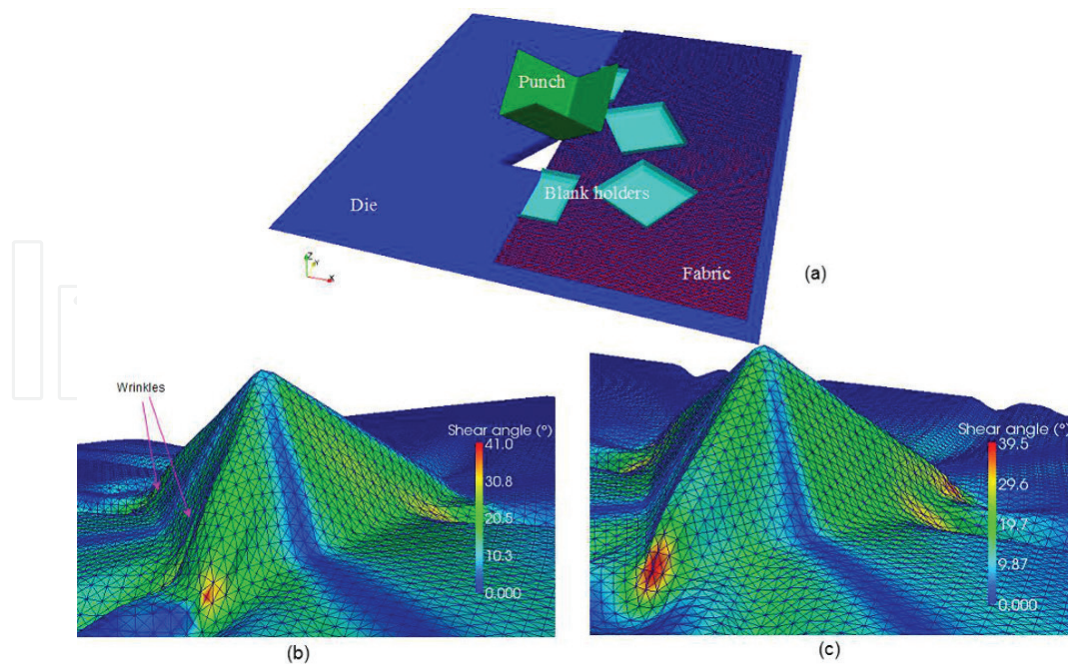

Figure 16. Numerical simulations of a corner fitting part forming. (a) Geometry model and mesh structure, (b) forming with a 0°/90° ply, and (c) forming with a −45°/+45° ply.

Tension in warp direction is assumed to be $T^{11} = C_1 \varepsilon_{11}$	Tensile stiffness in warp direction: $C_1 = 4600$ N/yarn
Tension in weft direction is assumed to be $T^{22} = C_2 \varepsilon_{22}$	Tensile stiffness in weft direction: $C_2 = 4600$ N/yarn
In-plane shear moment is assumed to be $M^s(\gamma) = k_1 \gamma + k_2 \gamma^3 + k_3 \gamma^5$	In-plane shear stiffness: $k_1 = 0.371$; $k_2 = -0.841$; $k_3 = 1.03$
Bending moment is assumed to be $M^1 = B_1 \chi_{11}$ in warp direction	Bending stiffness in warp direction: $B_1 = 0.5$ N mm
Bending moment is assumed to be $M^2 = B_2 \chi_{22}$ in weft direction	Bending stiffness in weft direction: $B_2 = 0.5$ N mm

Table 2. Mechanical behaviors of the textile composite fabric used in forming simulation.

4.1.2. Square box

Figures 17 and **18** present the square box forming with 0°/90° and −45°/45° plies by using blank-holder pressure of 0.05 MPa (a weak pressure). This pressure is applied homogenously on the blank-holder. The forming results correspond to a punch displacement of 85 mm. Due to the very weak intraply shearing effects, the in-plane shear angles inferior to 5° are measured on the upper surface and lateral surfaces of deformed 0°/90° ply (**Figure 17a**). On the contrary, the strong shear effects lead to an in-plane shear angle superior to 60°, which are observed on the corners of the square box and brings out the large wrinkles (**Figure 17b**). The in-plane shear angles between 25° and 35° are noted at two triangular zones shown in **Figure 18a**. Compared to these angles, the in-plane shear on the upper surface is negligible. As same as the forming of 0°/90° ply, the maximum in-plane shear angle can be observed on the corners (around 50°) and this strong in-plane shear effects lead to wrinkles (**Figure 18b**).
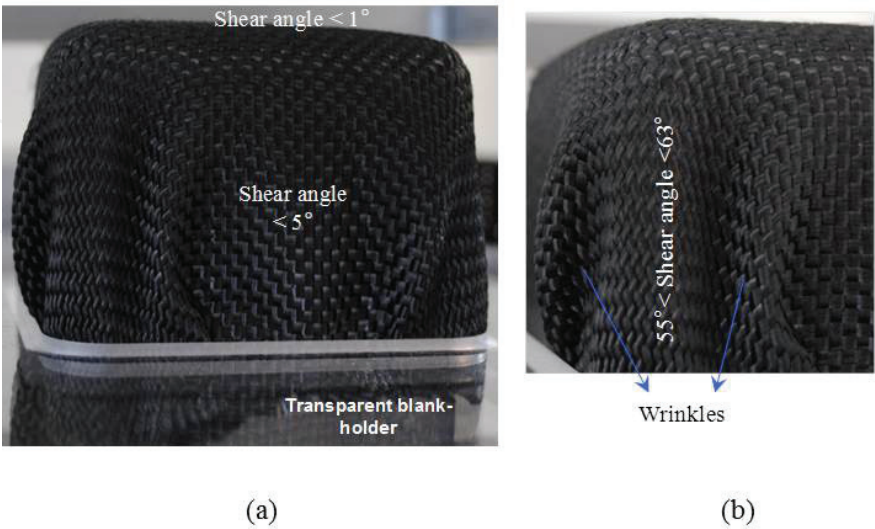

(a)   (b)

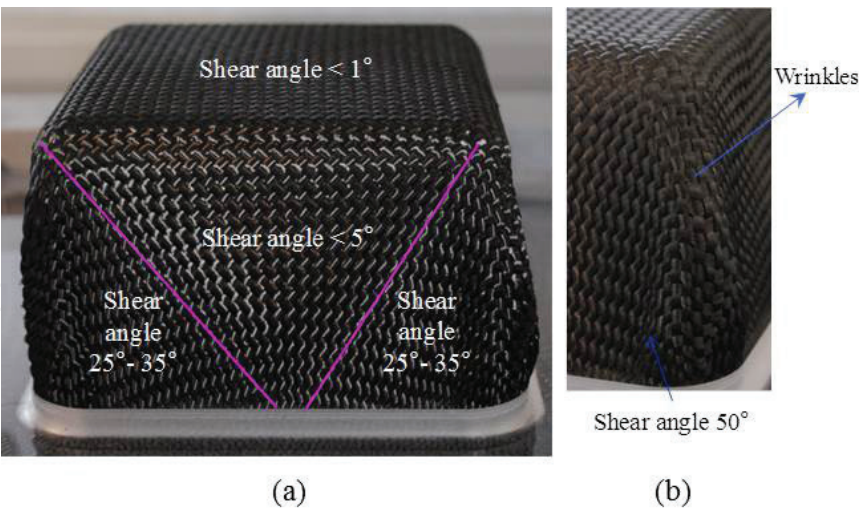**Figure 17.** Forming with 0°/90° ply at 0.05 MPa (a) and zoom on the corner zone (b).

Figure 18. Forming with −45°/45° ply at 0.05 MPa (a) and zoom on the corner zone (b).

The wrinkling depends strongly on the fabric characteristics. Therefore, the form and size of the wrinkles are different in the forming for 0°/90° and −45°/45° plies (**Figures 17b** and **18b**).

As one of the forming process parameters, the blank-holder force and the blank-holder shape and position can influence strongly on the wrinkling phenomena. A square box forming simulation with eight independent blank-holders is performed and shown in **Figure 19**. The same plain weave fabric presented in **Figures 17** and **18** is used in the forming simulation analysis. In this study, it is interesting to use the different pressure applied on different zones: a lower pressure in the corners or a higher pressure in the corners. As a higher pressure applied in the corners can lead to a more important tension and a more risk to create wrinkling and slippage of network, in the forming simulation a lower pressure of 0.05 MPa will be applied in the corners and a higher pressure of 0.2 MPa will be applied in the lateral sides (see **Figure 19**). The punch stroke is always 85 mm and the friction coefficient is 0.3.

The forming simulation results are shown in **Figures 20** and **21**. Wrinkles can be observed. Compared to the previous forming simulations, the distribution of in-plane shear angle is
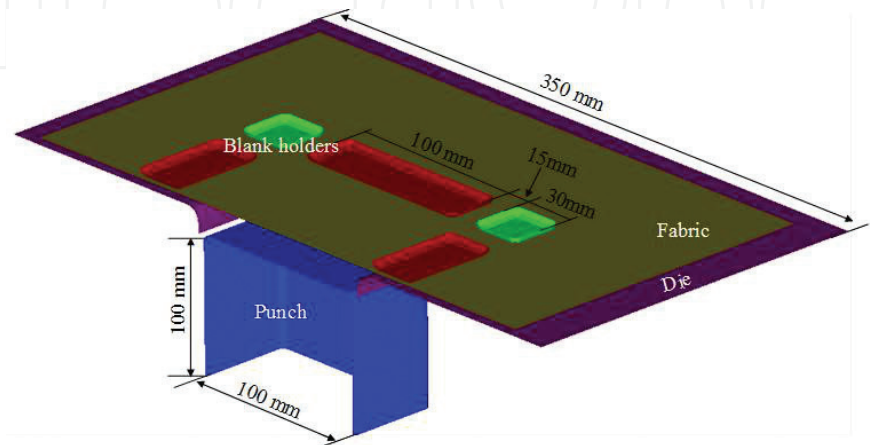

Figure 19. Geometry model and mesh structure of the square box forming with eight independent blank holders.
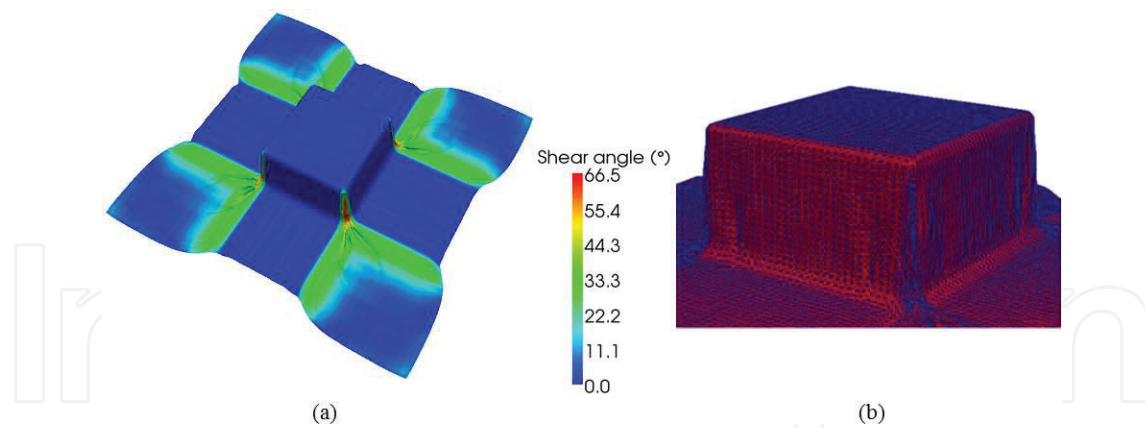
Figure 20. Square box forming simulation with eight independent blank holders for 0°/90° ply, (a) deformed ply and (b) zoom on the useful zone.
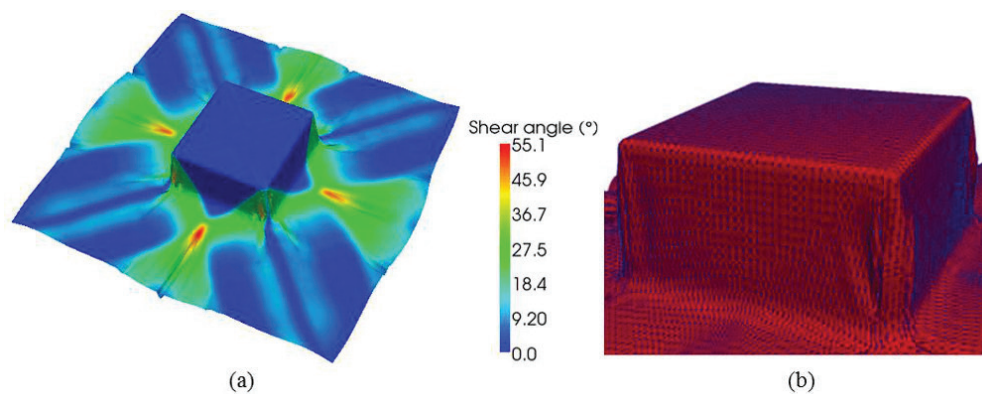

Figure 21. Square box forming simulation with eight independent blank holders for -45°/+45° ply, (a) deformed ply and (b) zoom on the useful zone.

very similar. Furthermore, the wrinkling phenomena are modified in the useful zone. Fewer wrinkles are noted in forming of 0°/90° ply but more on the corners of deformed −45°/45° ply. The forming simulation analyses emphasize that it is difficult to avoid the wrinkles in square box preforming with the considered textile reinforcement. Consequently, another manufacturing technology must be used to accomplish a product without wrinkles.

4.2. Surface 3D weaving

Compared to the bag weaving technique (the traditional weaving technique), two points should be developed in the surface 3D weaving method: assure the orientations and the continuity of fibers in each surface of corner fitting and square box.

4.2.1. 3D Corner fitting ply

The corner fitting 3D ply with the fiber direction of 0°/90° can be manufactured in the following main three steps. *The first step*: the first step concerns the yarns beaming and picking in the direction *X* as the traditional loom (**Figure 22a**). *The second step*: this step is still a traditional

weaving loom process. The yarns in the direction Y are weaved with the ones in the direction X to build face 1 (**Figure 22b**). *The third step*: the Z yarns are generated automatically by the free yarns in the directions X and Y. Then X and Y yarns are weaved with Z yarns automatically as shown in **Figure 22c**. The insertion of X and Y yarns is not rectilinear but in the path of "L." In this way, the two faces (faces 2 and 3) can be constructed in the same time.

The desired orientations of fiber are set by controlling the tow tension during the whole structuring (interlacing) process, which is a traditional solution used in the textile industry. The X and Y yarns produced in steps 1 and 2 are under tension control. In order to guarantee the same tension force on each tow, a spring is employed for each loop of carbon tow during step 3. All the X direction springs are connected together by a transverse bar self-controlled on tension, to assure global tension applied on the X tows. Each "L" weft (inserted tow during the step 3) is also tensioned
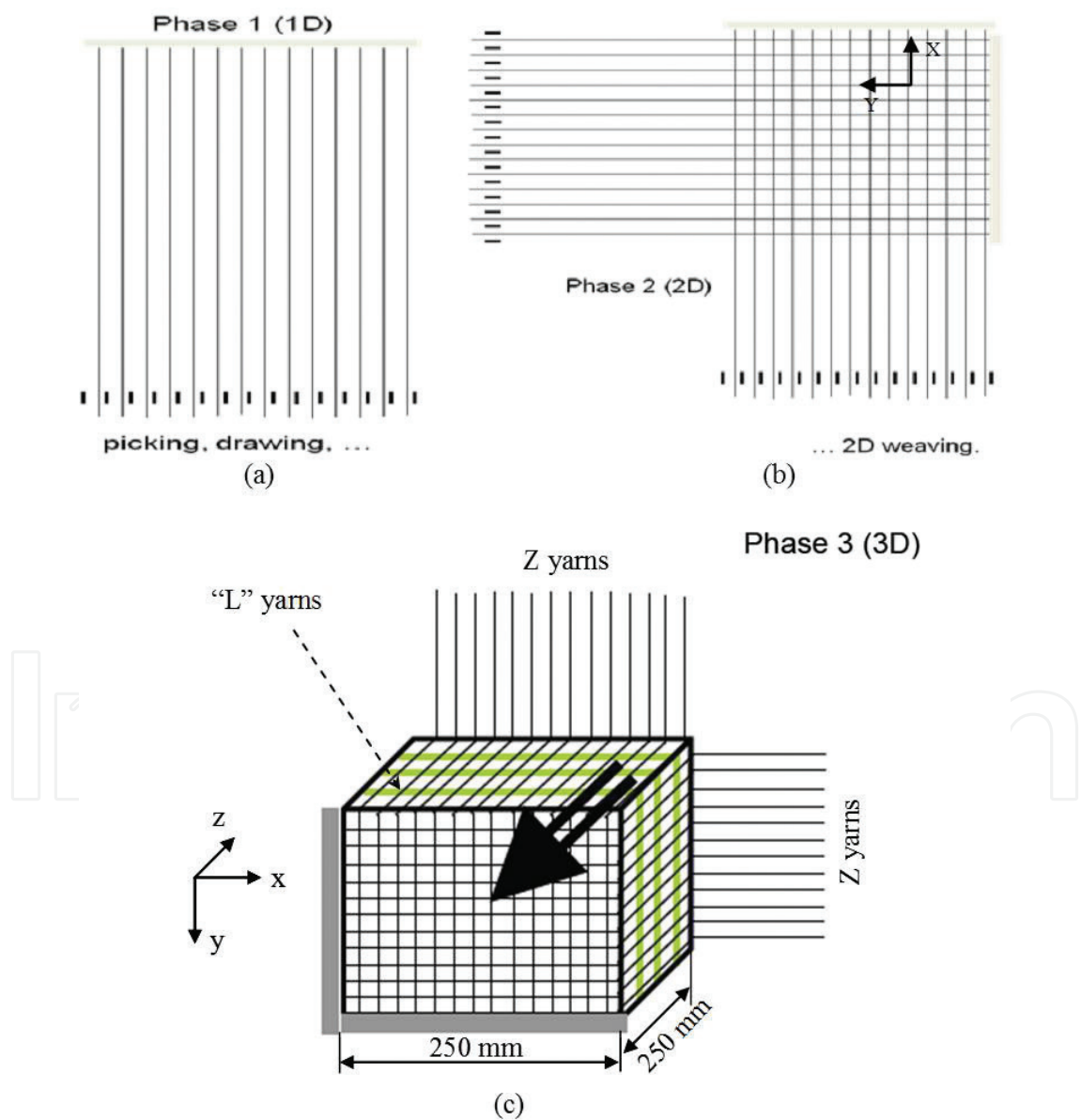

Figure 22. Different steps to manufacture the 3D corner fitting ply, (a) Phase 1 (1D), (b) Phase 2 (2D) and (c) Phase 3 (3D).

after its insertion between X and Y tows. Therefore, the tow is maintained in its right place and the desired orientations could be assured.

The −45°/45° corner fitting 3D ply can be produced in the similar way presented previously. The X and Y yarns are posed initially −45°/45°. Then the "L" yarns are weaved with XY yarns following −45° and 45° directions (**Figure 23**). The final 3D corner fitting plies with the fiber direction of 0°/90° and −45°/45° are shown in **Figure 24**. There are no wrinkles observed in these final 3D surface structures. The yarns in warp and weft directions stay perfectly perpendicular on the three faces and the continuity between faces is free from defects.
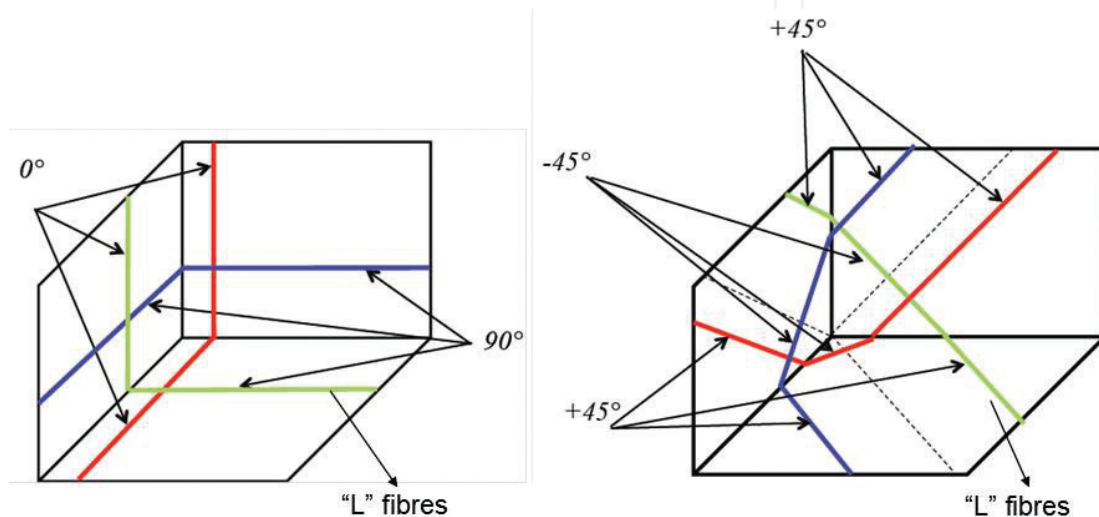

Figure 23. Directions of fibres in the 0°/90° and −45°/45° 3D corner fitting plies.

(a)   (b)

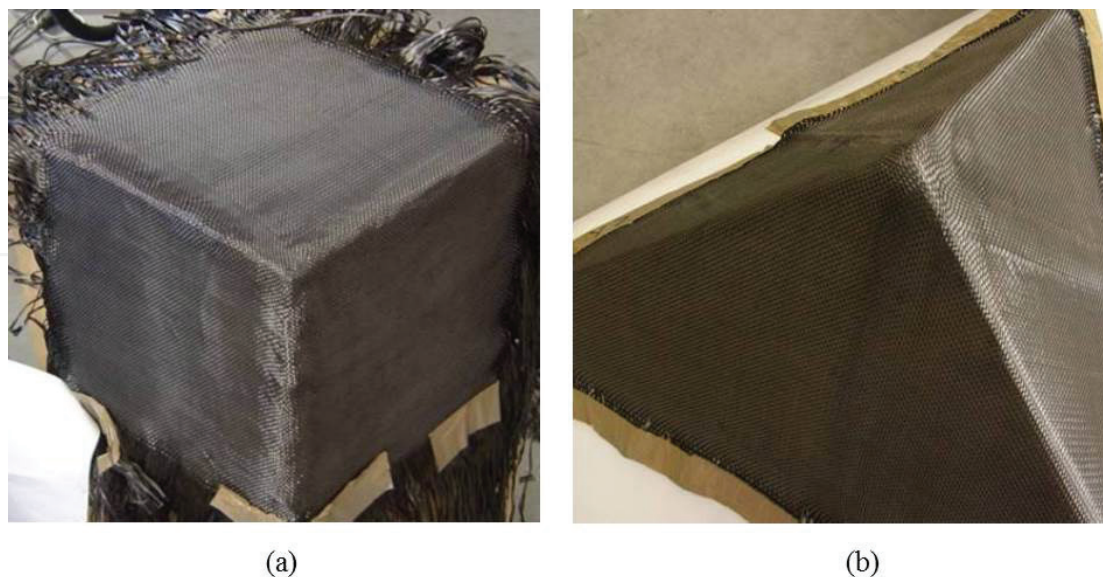**Figure 24.** The 3D corner fitting plies obtained by surface 3D weaving process, (a) [0°/90°] and (b) [−45°/45°] plies.

4.2.2. 3D square box ply

Figures 25 and **26** present the surface 3D weaving process for manufacturing automatically the 3D square box ply with the fiber orientation of 0°/90°. In the manufacturing of the 3D corner-fitting ply, the first step concerns the yarns drawing and picking in the direction X (**Figure 25a**). The second step is called 2D weaving, through this step the Y yarns are performed. In this case, the X and Y yarns build automatically the face 1 (upper surface of the square box) (see **Figure 25b**). Thanks to a transversal forming frame in Z-direction, the free X and Y yarns can be considered as Z yarns (**Figure 26a**). To produce faces 2–5, the last X or Y yarn is used to weave with the Z yarns (see **Figure 26b**). The last two X or Y yarns are chosen on opposite faces and turn round to weave more rapidly with the Z yarns. The insertion of XY yarns is nonrectilinear but in a "rectangle" path (**Figure 26b** and **c**). In this way, the lateral faces (faces 2–5) can be constructed together. The warp and weft yarns on the lateral faces are not strictly perpendicular due to the yarn's width (**Figure 26c**). This deviation will be reduced by the increase of the dimensions of the box.

As for 3D corner fitting ply, the fibers' orientations must be well controlled. The manufactured 3D textile square box is shown in **Figure 27**. Some local defects due to manipulation of the ply are observed in the figure, these local defects can be absolutely avoided. No wrinkles on the faces and at the edges can be noted. The warp and weft yarns are perfectly under control and the continuity between faces is properly implemented.

The 0°/90° and −45°/45° 3D plies are produced and then laminated together. In this case, it should adapt the dimensions of final composite by changing warp and weft densities or by adding/removing one tow. The laminated corner fitting or square box plies can be manufactured by the RTM process to obtain a composite piece (**Figure 28**). Surface 3D weaving technique

(a)

(b)

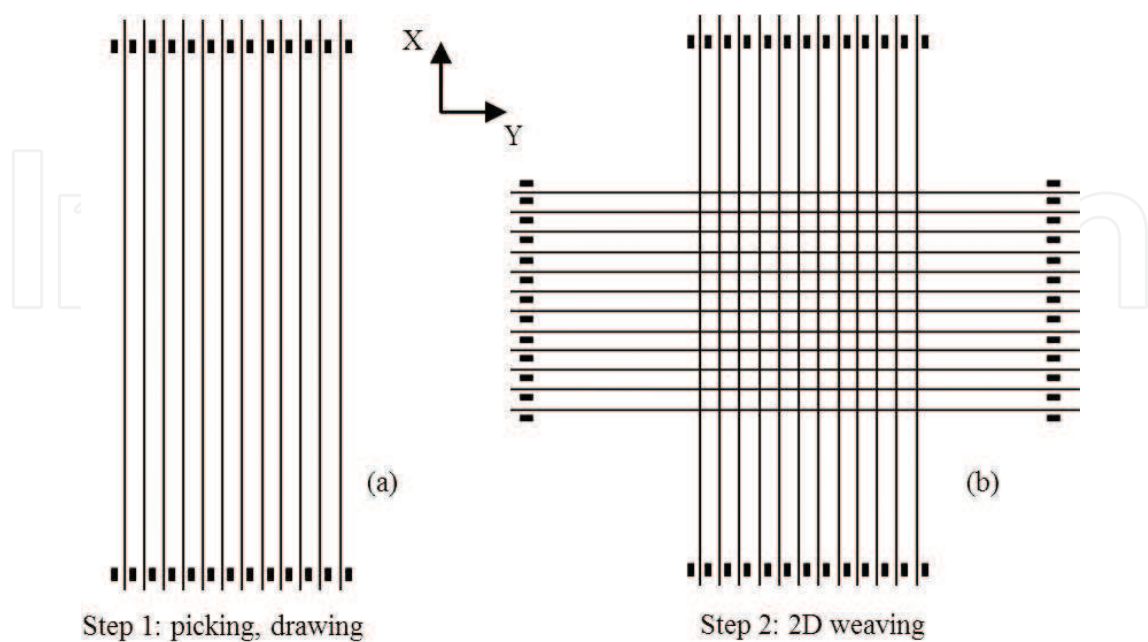Step 1: picking, drawing

Step 2: 2D weaving

Figure 25. The first two steps to produce the 3D square box ply, (a) picking and drawing and (b) 2D weaving.
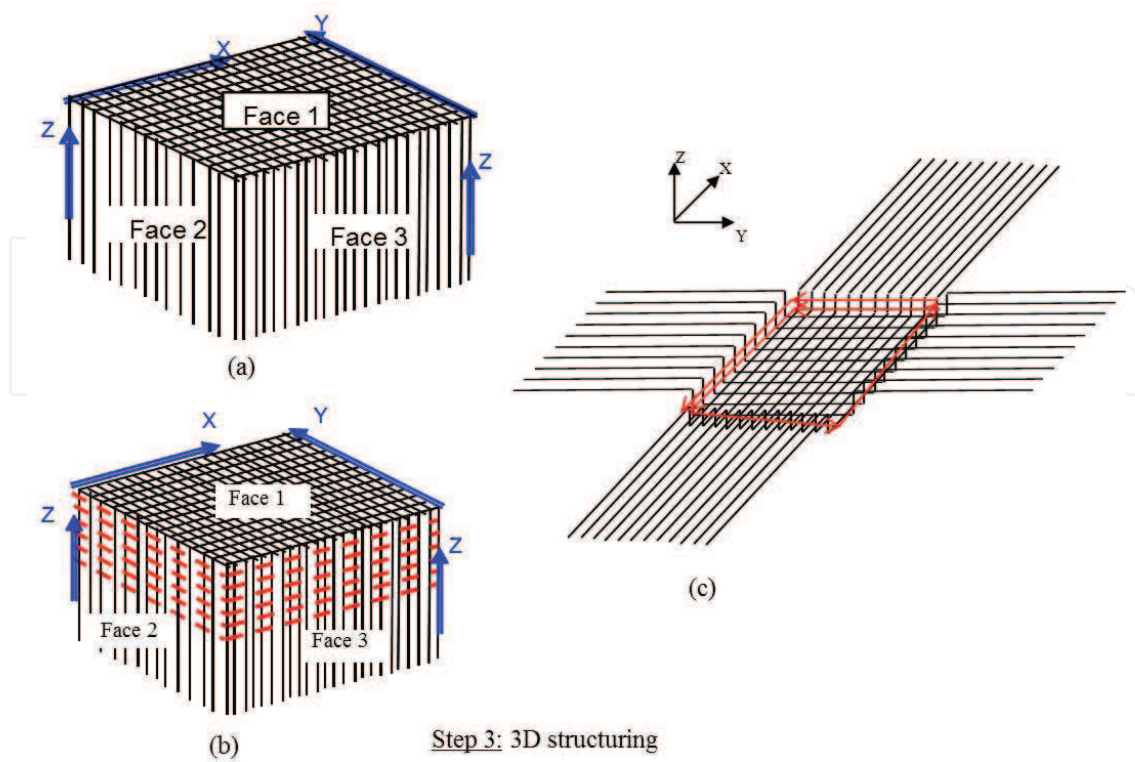
Figure 26. The 3D structuring step in surface 3D weaving process, (a) Z yarns, (b) face 2- face 5 and (c) weaving in a "rectangle" path.
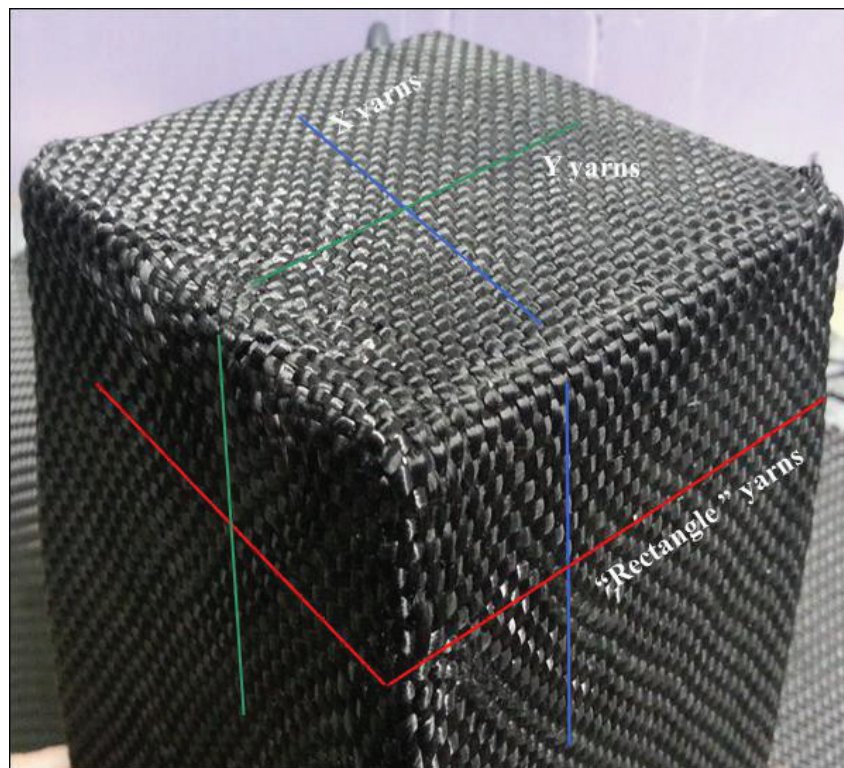

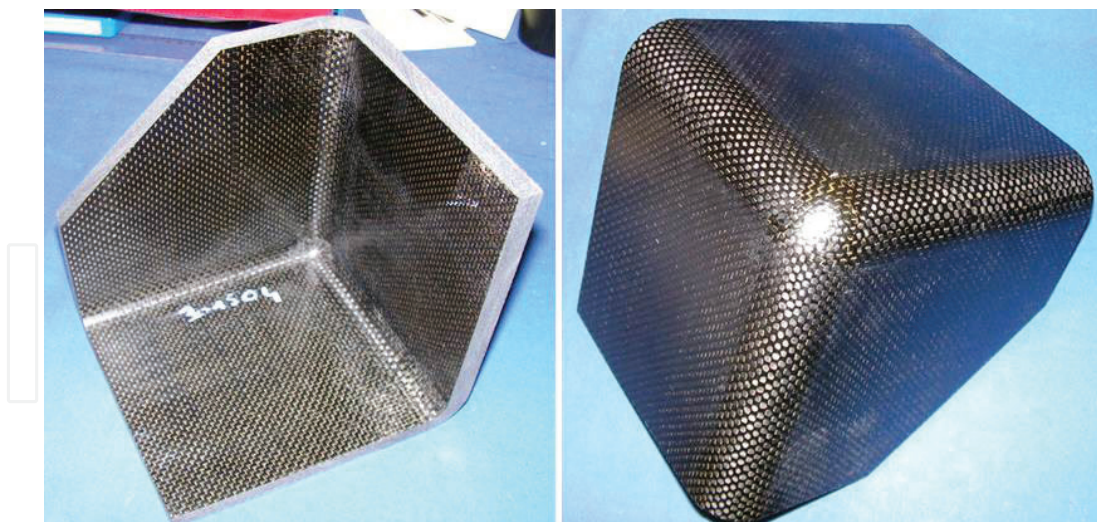**Figure 27.** 3D square box ply obtained by surface 3D weaving.

Figure 28. Final corner fitting composite part.

is defined in another way to design and produce the textile reinforcement for composite pre-forms when the shape is strongly double curved. Through this technique, it is possible to make a lighter composite part, nevertheless the conception and implementation are time-consuming. The main advantage of this new technique is the control throughout the process of the orientation of the carbon tow. The preform is free from any local or global misalignment. Moreover, the manufacture of the preform is made in a single operation (divided into three simple steps) very similar to traditional weaving. This is a direct process to obtain the 3D preform. Moreover, this new technique limits the tows' damage as they are less stressed than by the weaving technique and performing process.

5. Conclusions

The different promising textile reinforcements based on the advanced textile technologies for composite manufacturing have been presented in this chapter. The reinforcements (structure, manufacturing process, etc.) influence strongly on the properties of final composite materials. The innovation of the textile reinforcement structure is always a challenge in the composite research field. The 2D fabrics are employed frequently in the manufacturing of composite materials by forming/thermoforming processes. The double-curved shape forming can possibly lead to defects; it depends strongly on the forming parameters (tool loads, blank-holder forces, temperature, etc.). It is fast and more efficient, in particular for the manufacturing of multilayer laminates and interlock fabrics. The thick fabric can be used to produce thicker, lighter, and stronger composite parts. The through-the-thickness reinforcement of 3D structures is a promising attempt to overcome several problems. As one type of 3D textile reinforcements, the tufted 3D fabric is very interesting for the manufacturing of advanced composite part. Delamination can be reduced due to the existence of transverse reinforcement (reinforced yarns through-the-thickness), and the impact resistance and the damage tolerance are relatively strengthened. Compared to the stitch and interlock techniques, the tufting is

user-friendly, more rapid, and low-cost process. The tufting yarns can minimize the interply sliding and the defects (e.g., wrinkles and misalignment) during the forming.

Compared to the textile reinforcement forming, the yarn directions can be well controlled for the surface 3D ply obtained by 3D surface weaving. The 3D surface weaving is a direct way to obtain 3D reinforcement. The wrinkling can be avoided completely and the local permeability of the 3D ply is homogenous, which is a big advantage for the resin injection/infusion stage during the liquid composite molding processes. It should be pointed out here that textile reinforcement forming is more developed. It is employed widely for both dry textile reinforcements and prepregs materials. To avoid the forming defects, it is important to predict the feasible conditions of composites forming, for example, by numerical simulation.

Author details

Peng Wang*, Xavier Legrand and Damien Soulat

*Address all correspondence to: peng.wang@ensait.fr

University of Lille, ENSAIT, GEMTEX, Roubaix, France

References

[1] Walther J, Simacek P, Advani SG. The effect of fabric and fiber tow shear on dual scale flow and fiber bundle saturation during liquid molding of textile composites. International Journal of Material Forming. 2012;**5**(1):83-97

[2] Trochu F, Ruiz E, Achim V, Soukane S. Advanced numerical simulation of liquid composite molding for process analysis and optimization. Composites Part A. 2006;**37**:890-902

[3] Swery EE, Allen T, Comas-Cardona S, Govignon Q, Hickey C, Timms J, et al. Efficient experimental characterisation of the permeability of fibrous textiles. Journal of Composite Materials. 2016;**50**(28):4023-4038

[4] Lomov S.V. Modelling the geometry of textile reinforcements for composites: WiseTex. In: Boisse P, editor. Composite Reinforcements for Optimum Performance. 1st ed. Woodhead Publishing; 2011. p. 200-238. DOI: http://doi.org/10.1533/9780857093714.2.200

[5] Long AC. Composites Forming Technologies. New York, NY: CRC Press; 2007

[6] Christos K. Design and Analysis of Composite Structures: With Application to Aerospace structures. New York, NY: Wiley; 2010

[7] Allaoui S, Hivet G, Soulat D, Wendling A, Ouagne P, Chatel S. Experimental preforming of highly double curved shapes with a case corner using an interlock reinforcement. International Journal of Material Forming. 2014;**7**(2):155-165

[8]   Allaoui S, Cellard C, Hivet G. Effect of inter-ply sliding on the quality of multilayer interlock dry fabric preforms. Composites Part A. 2015;**68**:336-345

[9]   Harrison P, Gomes R, Curado-Correia N. Press forming a 0/90 cross-ply advanced thermoplastic composite using the double-dome benchmark geometry. Composites Part A. 2013;**54**:56-69

[10] Boisse P, Aimène Y, Dogui A, Dridi S, et al. Hypoelastic, hyperelastic, discrete and semi-discrete approaches for textile composite reinforcement forming. International Journal of Material Forming. 2010;**3**:1229-1240

[11] Hamila N., Boisse P. Simulations of textile composite reinforcement draping using a new semi-discrete three node finite element. Composites Part B. 2008;**39**:999-1010

[12] Dufour C, Wang P, Boussu F, Soulat D. Experimental investigation about stamping behavior of 3D warp interlock composite preforms. Applied Composite Materials. 2014;**21**(5): 725-738

[13] Tephany C, Soulat D, Gillibert J, Ouagne P. Influence of the non-linearity of fabric tensile behavior for preforming modeling of a woven flax fabric. Textile Research Journal. 2016;**86**(6): 604-617

[14] Pazmino J, Carvelli V, Lomov SV. Formability of a non-crimp 3D orthogonal weave E-glass composite reinforcement. Composites Part A. 2014;**61**:76-83

[15] Allaoui S, Boisse P, Chatel S, Hamila N, Hivet G, Soulat D, et al. Experimental and numerical analyses of textile reinforcement forming of a tetrahedral shape. Composites Part A. 2011;**42**(6):612-622

[16] Boisse P, Zouari B, Gasser A. A mesoscopic approach for the simulation of woven fiber composite forming. Composites Science and Technology. 2005;**65**(3-4):429-436

[17] Syerko E, Comas-Cardona S, Binetruy C. Models for shear properties/behavior of dry fibrous materials at various scales: A review. International Journal of Material Forming. 2015;**8**:1-23

[18] Potter K, Khan B, Wisnom M, Bell T, Stevens J. Variability, fiber waviness and misalignment in the determination of the properties of composite materials and structures. Composites Part A. 2008;**39**:1343-1354

[19] Bloom LD, Wang J, Potter KD. Damage progression and defect sensitivity: An experimental study of representative wrinkles in tension. Composites Part. 2013;**45**:449-458

[20] Ouagne P, Soulat D, Moothoo J, Capelle E, Gueret S. Complex shape forming of a flax woven fabric; analysis of the tow buckling and misalignement defect. Composites Part A. 2013;**51**:1-10

[21] Ouagne P, Soulat D, Tephany C, Gillibert J. Measurement of the appearance and growth of tow buckling defect in the frame of complex shape manufacturing process by using fringe projection technique. Strain. 2016;**52**(6):559-569

[22] Warren KC, Lopez-Anido RA, Goering J. Experimental investigation of three-dimensional woven composite. Composites Part A. 2015;**73**:242-259

[23] Wang P, Hamila N, Boisse P. Thermoforming simulation of multilayer composites with continuous fibers and thermoplastic matrix. Composites Part B. 2013;**52**:127-136

[24] Bel S, Hamila N, Boisse P, Dumont F. Finite element model for NCF composite reinforcement preforming: Importance of inter-ply sliding. Composites Part A. 2012;**43**:2269-2277

[25] Mulvihill DM, Sutcliffe MPF. Effect of tool surface topography on friction with carbon fibre tows for composite fabric forming. Composites Part A. 2017;**93**:199-206

[26] Liang B, Hamila N, Peillon M, Boisse P. Analysis of thermoplastic prepreg bending stiffness during manufacturing and of its influence on wrinkling simulations. Composites Part A. 2014;**67**:111-122

[27] Bhattacharyya D, editor. Composite sheet Forming. 1st ed. Elsevier Science; 1977.

[28] Potter K., Ward C. Draping processes for composites manufacture. In: Boisse P, editor. Advances in Composites Manufacturing and Process Design. 1st ed. Woodhead Publishing; 2015. P. 93-109. DOI: http://doi.org/10.1016/B978-1-78242-307-2.00005-1

[29] Capelle E, Ouagne P, Soulat D, Duriatti D. Complex shape forming of flax woven fabrics: Design of specific blank-holder shapes to prevent defects. Composites Part B. 2014;**62**:29-36

[30] Omrani F, Wang P, Soulat D, Ferreira M, Ouagne P. Analysis of the deformability of flax-fibre nonwoven fabrics during manufacturing. Composites Part B. 2016. DOI: http://dx.doi.org/10.1016/j.compositesb.2016.11.003

[31] Duhovic M, Mitschang P, Bhattacharyya D. Modeling approach for the prediction of stitch influence during woven fabric draping. Composites Part A. 2011;**42**(8):968-978

[32] Mathieu S, Hamila N, Bouillon F, Boisse P. Enhanced modeling of 3D composite preform deformations taking into account local fiber bending stiffness. Composites Science and Technology. 2015;**117**:322-333

[33] Omrani F, Wang P, Soulat D, Ferreira M, Mechanical properties of flax-fibre reinforced preforms and composites: Influence of the type of yarns on multi-scale characterizations. Composites Part A. 2017;**93**:72-81

[34] Jacquot PB, Wang P, Soulat D, Legrand X. Analysis of the preforming behavior of the braided and woven flax/polyamide fabrics. Journal of Industrial Textiles. 2016;**46**(3): 698-718

[35] Risicato JV, Kelly F, Soulat D, Legrand X, Trumper W, Cochrane C, et al. A complex shaped reinforced thermoplastic composite part made of commingled yarns with integrated sensor. Applied Composite Material. 2015;**22**(1):81-98

[36] Kazemahvazi S, Khokar N, Hallstrom S, Wadley HNG, Deshpande VS. Confluent 3D-assembly of fibrous structures. Composites Science and Technology. 2016;**127**:95-105

[37] Mouritz AP, Bannister MK, Falzon PJ, Leong KH. Review of applications for advanced three-dimensional fiber textile composites. Composites Part A. 1999;**30:**1445-1461

[38] Kamiya R, Cheeseman BA, Popper P, Chou TW. Some recent advances in the fabrication and design of three-dimensional textile preforms: A review. Composite Science and Technology. 2000;**60**:33-47

[39] Potluri P, Hogg P, Arshad M, Jetavat D, Jamshidi P. Influence of fiber architecture on impact damage tolerance in 3D woven composites. Applied Composite Material. 2012;**19**(5): 799-812

[40] Boussu F, Cristian I, Nauman S. General definition of 3D warp interlock fabric architecture. Composites Part B. 2015;**81**:171-188

[41] Rahali Y, Goda I, Ganghoffer JF. Numerical identification of classical and nonclassical moduli of 3D woven textiles and analysis of scale effects. Composites Structures. 2016;**135**:122-139

[42] Saleh MN, Lubineau G, Potluri P, Withers PJ, Soutis C. Micro-mechanics based damage mechanics for 3D orthogonal woven composites: Experiment and numerical modeling. Composites Structures. 2016;**156**:115-124

[43] Gras R, Leclerc H, Roux S, Otin S, Schneider J, Périé JN. Identification of the out-of-plane shear modulus of a 3D woven composite. Experimental Mechanics. 2013;**53**(5):719-730

[44] Naouar N, Vidal-Salle E, Schneider J, Maire E, Boisse P. 3D composite reinforcement meso F.E. analyses based on X-ray computed tomography. Composites Structures. 2015;**132**:1094-1104

[45] Pegorin F, Pingkarawat K, Daynes S, Mouritz AP. Influence of z-pin length on the delamination fracture toughness and fatigue resistance of pinned composites. Composites Part B. 2015;**78**:298-307

[46] Chen X, Taylor WL, Tsai LJ. An overview on fabrication of three-dimensional woven textile preforms for composites. Textile Research Journal. 2011;**81**:932-944

[47] Mouritz AP, Leong KH, Herszberg I. A review of the effect of stitching on the in-plane mechanical properties of fiber-reinforced polymer composites. Composites Part A. 1997;**28A**: 979-991

[48] Dell'Anno G, Treiber J, Partridge I. Manufacturing of composite parts reinforced through-thickness by tufting. Robotics and Computer-Integrated Manufacturing. 2016;**37**:262-272

[49] Kyosev Y. Geometrical modeling and computational mechanics tools for braided structures. In: Kyosev Y, editor. Advances in Braiding Technology Specialized Techniques and Applications. 1st ed. Woodhead Publishing; 2016. P. 501-519. DOI: http://doi.org/10.1016/B978-0-08-100407-4.00021-1

[50] Abounaim M, Diestel O, Hoffmann G, Cherif C. High performance thermoplastic composite from flat knitted multi-layer textile preform using hybrid yarn. Composites Science and Technology. 2011;**71**(4):511-519

[51] NASA Technical Reports Server (NTRS) 19970017583: Handbook of Analytical Methods for Textile Composites, 1997.

[52] Mouritz AP. Flexural properties of stitched GRP laminates. Composites Part A. 1996;**27**(7): 525-530

[53] Mouritz AP, Cox BN. A mechanistic approach to the properties of stitched laminates. Composites Part A. 2000;**31**(1):1-27

[54] Koh T, Isa M, Chang P, Mouritz AP. Improving the structural properties and damage tolerance of bonded composite joints using z-pins. Journal of Composite Materials. 2012;**46**(26):3255-3265

[55] Pérès P., Desmars B., Léard J.P. Composite behavior of assemblies with AEROTISS® 03S technology. In: 16th International Conference on Composite Materials; July 8-13; Kyoto, Japan. 2007.

[56] Ko F.K., Du G.W. Textile Preforming. In: Peters S.T., editor. Handbook of Composites. Springer; 1998. p. 397-424.

[57] Fukuta K, Aoki E, Nagatsuka Y. 3-D fabrics for structural composites. In: 15th Textile Research Symposium; Philadelphia, PA. 1986

[58] Henao A, Carrera M, Miravete A, Castejon L. Mechanical performance of through-thickness tufted sandwich structures. Composite Structures. 2010;**92**:2052-2059

[59] Vanclooster K., Lomov S.V., Verpoest I. On the formability of multi-layered fabric. In: 17th International Conference on Composite Materials; July 27-31; Edinburgh, UK. 2009.

[60] ten Thije RHW, Akkerman R. A multi-layer triangular membrane finite element for the forming simulation of laminated composites. Composites Part A. 2009;**40**:739-753

[61] Boisse P, Hamila N, Vidal-Sallé E, Dumont F. Simulation of wrinkling during textile composite reinforcement forming. Influence of tensile in-plane shear and bending stiffnesses. Composites Science and Technology. 2011;**71**(5):683-692

[62] Prodromou AG, Chen J. On the relationship between shear angle and wrinkling of textile composite performs. Composites Part A. 1997;**28A**:491-503

[63] Kawabata S, Niwa M, Kawai H The finite deformation theory of plain weave fabrics part I: The biaxial deformation theory. Journal of the Textile Institute. 1973;**64**(1):21-46